JOURNAL OF SOLID STATE CHEMISTRY **123,** 140–149 (1996)
ARTICLE NO. 0162

Na, K, Rb, and Cs Exchange in Heulandite Single-Crystals: X-Ray Structure Refinements at 100 K

Ping Yang and Thomas Armbruster[1]

Laboratorium für chem. und miner. Kristallographie, Universität Bern, Freiestrasse 3, CH-3012 Bern, Switzerland

Received October 5, 1995; in revised form January 22, 1996; accepted January 25, 1996

The crystal structures of Na-, K-, Rb-, and Cs-exchanged varieties of the zeolite heulandite with the simplified composition $M_9^+Al_9Si_{27}O_{72} \cdot nH_2O$ were studied by single-crystal X-ray diffraction at 100 K. The structure refinements of Na-, K-, and Rb-exchanged heulandite were performed in space group $C2/m$ with resultant R values of 3.8, 3.0, and 4.9%, respectively. Cs-exchanged heulandite was refined in space group $C\bar{1}$, yielding an R value of 3.4%. X-ray single-crystal data of the Cs-exchanged variety indicated that many reflections of type $h\ k\ l$ were not equivalent to $h\ -k\ l$ as expected for monoclinic symmetry. With increasing radius of the incorporated channel cations, the b axis increases from 17.93 to 18.09 Å leading to a slight widening of the channels. The number of H_2O molecules also decreases with increasing cation radius due to space limitations. Three general cation positions (II-1, *C*3, and *B*4) were found in the four exchanged heulandite samples. For Rb- and Cs-exchanged crystals, the additional cation site *A*2 occurs. In Cs-exchanged heulandite symmetry lowering is due to partial Si, Al ordering in the framework accompanied with a more asymmetric arrangement of channel Cs. Only if heavy elements in the channels are present the symmetry information of the framework is enforced, thus partial Si, Al ordering can be resolved.

INTRODUCTION

Heulandite-type zeolites comprise heulandite and clinoptilolite with the simplified formulas $(Na, K)Ca_4Al_9Si_{27}O_{72} \cdot 24H_2O$ and $(Na, K)_6(Al_6Si_{30}O_{72}) \cdot 20H_2O$ (1). Both minerals represent naturally occurring zeolites with a high degree of Si, Al disorder (2, 3). The crystal structure (space group $C2/m$, $a \approx 17.67$, $b \approx 17.87$, $c \approx 7.41$ Å, $\beta \approx 116.39°$) exhibits three types of structural channels confined by tetrahedral ring systems. Ten-membered *A-rings* and eight-membered *B-rings* confine the A and B channels running parallel to the c axis. Eight-membered *C-rings* border C channels running parallel to [100] and [102] (4). Two eight-membered rings of channel B and two additional eight-membered rings of channel C form cage I. Two ten-membered rings of channel A and two eight-membered rings of channel C form cage II.

Zeolites of the heulandite structure type are widely occurring minerals which are available as large masses to be excavated at low cost in quarries. This type of natural zeolite has been used for the removal of radioactive Cs^+ and Sr^{2+} from low level waste streams of nuclear power stations and for extraction of ammonium from sewage because of heulandites excellent selectivity for cation exchange and adsorption (5). Galli *et al.* (6) studied the structures of K-exchanged heulandite at elevated temperatures. It was found that K^+ is strongly disordered and dehydration takes place at 373 K accompanied by a deformation of the framework. Smyth *et al.* (7) refined the single-crystal structure of a partially Cs-exchanged clinoptilolite sample in space group $C2/m$. Cs^+ occupies split positions that are not related to the cation positions in the natural Na^+-, K^+-, and Ca^{2+}-bearing sample. Petrov *et al.* (8, 9) performed an X-ray powder study of Cs- and Ba-exchanged clinoptilolite in space group $C2/m$. An additional Cs^+ position, not reported by Smyth *et al.* (7), was located owing to the high degree of Cs^+ incorporation in this Cs-exchanged clinoptilolite. In Ba-exchanged clinoptilolite Ba^{2+} resides in the eight-membered rings of channel C. Bresciani-Pahor *et al.* (10, 11) reported the structures of a partially and a fully Ag-exchanged heulandite. Ag^+ occupies the positions analogous to Ca^{2+} and Na^+ in natural samples (2, 3). In addition, a new site with a low occupancy was assigned to Ag^+. The authors (10, 11) suggested that some Ag^+ ions were statistically disordered in the zeolite pores because the total amount of Ag^+ located by X-ray refinement was significantly lower than that determined by chemical analysis. Gunter *et al.* (12) refined the structure of Pb-exchanged heulandite in space group Cm while they noted that the single-crystal diffraction pattern clearly contradicted a centric space group because reflections of the type $h\ k\ l$ and $-h\ -k\ -l$ were not equivalent. The reason for the symmetry lowering is that in Pb-exchanged heulandite Pb^{2+} preferred an ordered position in agreement with Cm but in contrast to $C2/m$ symmetry. Alberti and Vezzalini (13) and Armbruster and co-workers (14, 15) studied the dehy-

[1] To whom correspondence should be addressed.

0022-4596/96 $18.00

dration mechanism of heulandite by single-crystal X-ray methods. Hambley and Taylor (16) performed a neutron diffraction study of natural and partially dehydrated heulandite where also H positions of the H_2O molecules were found. The dehydration of heulandite is accompanied by cation diffusion within the channels and by a compression of the channel system.

The aim of this article is to find some general rules concerning channel site preference depending on ionic radii through a systematic structure study of alkali-exchanged heulandites. As starting material a Ca-rich natural sample is applied because the substitution $2M^+ \rightarrow Ca^{2+}$ guarantees high channel populations. Low temperature (100 K) was chosen for the structural study to minimize dynamic disorder phenomena. We also hoped that the systematic study could reveal some new information on the framework of heulandite because as exchanged cations become heavier, symmetry information of the framework is also enforced.

TABLE 1
Data Collection Conditions

Sample	Na-exchanged	K-exchanged	Rb-exchanged	Cs-exchanged
Crystal size	0.3×0.3×0.1	0.4×0.4×0.1	0.6×0.4×0.1	0.2×0.2×0.1
Space group	C2/m	C2/m	C2/m	$C\bar{1}$
Radiation		MoKα		
Scan type		ω		
Scan width	1.5	2.5	1.5	1.5
a (Å)	17.677(2)	17.636(12)	17.686(6)	17.760(4)
b (Å)	17.931(1)	17.934(5)	18.007(7)	18.095(2)
c (Å)	7.426(1)	7.397(4)	7.403(4)	7.428(1)
α°				89.91(1)
β°	116.47(1)	116.00(5)	116.15(4)	115.93(1)
γ°				90.18(1)
V(Å³)	2107.0(5)	2103(2)	2116(1)	2146.8(7)
Maximum θ°	30	25	25	25
Measured reflections	5412	3835	3837	4697
Unique reflections	3040	1904	1913	3643
Observed reflections	2588	1648	1695	3224
No. of parameters	240	209	207	358
R_w(%)	2.1	1.2	2.2	0.7
R(%)	3.8	3.0	4.9	3.4
R_e(%)	4.4	4.2	5.7	4.3

Note. $R = \Sigma \, | \, |F_{obs}| - |F_{calc}| \, | / \Sigma | F_{obs}|$, $R_w = (\Sigma \, w(|F_{obs}| - |F_{calc}|)^2 / \Sigma \, w \, |F_{obs}|^2)^{1/2}$.

EXPERIMENTAL

Large single crystals (up to 5 mm in dimension) of a natural heulandite from Nasik, India (17) were broken and sieved to give 0.1 ~ 0.5 mm samples and were subsequently placed in 2 *M* NaCl solution. The exchange reaction lasted 5 weeks at 373 K, and then the crystals were transferred to a Teflon-coated autoclave and heated at 423 K for another week. During the exchange process, the solution was renewed several times. After the exchange reaction, the sample was filtered, washed with distilled water, and dried in air at room temperature yielding Na-exchanged heulandite as a precursor phase. K-, Rb-, and Cs-exchanged heulandite were obtained by exchanging Na-exchanged heulandite with corresponding 2 *M MC*l solutions in a Teflon-coated autoclave at 423 K for 2 or 3 weeks, renewing the solutions 2 to 3 times. After exchange the samples were treated as the Na-exchanged heulandite.

Compositions of the natural heulandite and the exchanged samples were determined by a CAMECA SX50 electron microprobe operating at 20 kV and 20 nA beam current and defocused beam diameter of about 20 μm to prevent sample destruction and channel cation loss. Amelia albite was used as standard for Na, Al, and Si, orthoclase for K, and anorthite for Ca. Synthesized $RbVO_3$ and $CsVO_3$ (18) were used as standards for Rb and Cs.

Single-crystal X-ray data were obtained at 100 K with an Enraf-Nonius CAD-4 diffractometer (graphite-monochromatized Mo$K\alpha$ radiation), where low temperature was achieved with a conventional liquid nitrogen cooling device. Cell dimensions were obtained from 10 to 12 reflections with $20° < 2\theta < 35°$. Reflections were recorded for at least a half sphere of reciprocal space up to $\theta = 25°$. For Cs-exchanged heulandite a full sphere was collected up to 15°. All data were empirically corrected for absorption by using ψ scans. Data reduction including background and Lorenz-polarization correction was performed using the SDP program library (19). The program SHELXTL (20) using neutral atom scattering factors was applied for the structure refinements weighted $1/\sigma^2$. Due to the strong Si, Al disorder, tetrahedral positions were refined with Si scattering factors which has only a minor bearing on a atomic displacement parameters (21). Atomic coordinates of Na-exchanged heulandite (12) were used as starting parameters for the refinements. Cations in the structural pores were assigned according to electron density maxima and reasonable distances of the assumed site to neighboring oxygen atoms of the framework and water molecules. Anisotropic displacement parameters were refined for framework atoms, highly populated extra-framework cations, and H_2O molecules. Experimental details are summarized in Table 1.

For convenience, we label the general extra-framework cation positions in the rings by an italic letter referring to the surrounding tetrahedral ring system and cation positions in the cages by a Roman number. The positions are continuously numbered. Individual cations are labelled by their chemical symbols accompanied with numbers and disordered positions with an additional prime (′). Channel H_2O molecule are designated W.

RESULTS

The composition of the natural starting material is $Ca_{3.54}Na_{0.96}K_{0.09}Al_{8.62}Si_{27.51}O_{72} \cdot n \; H_2O$. Electron microprobe analysis and structure refinements indicated that the Na-treated sample was not completely exchanged and 1.5 Ca per formula unit (pfu) persisted in the structural channels.

TABLE 2
Framework Positional Parameters of Na-, K-, and Rb-Exchanged Heulandite

sample	atom	x/a	y/b	z/c	Beq
Na-	T1	0.17931(3)	0.17025(3)	0.09656(8)	0.948(8)
K-	T1	0.17999(5)	0.16907(5)	0.1019(1)	1.01(1)
Rb-	T1	0.17932(8)	0.17018(8)	0.1005(2)	0.83(2)
Na-	T2	0.28612(5)	0.08907(5)	0.4982(1)	1.12(1)
K-	T2	0.28612(5)	0.08907(5)	0.4982(1)	1.12(1)
Rb-	T2	0.28493(9)	0.08907(8)	0.4960(2)	1.01(2)
Na-	T3	0.29150(3)	0.31041(3)	0.28324(8)	0.940(8)
K-	T3	0.29382(5)	0.30981(5)	0.2857(1)	1.03(1)
Rb-	T3	0.29412(8)	0.30910(8)	0.2871(2)	0.86(2)
Na-	T4	0.06468(3)	0.29752(3)	0.41023(8)	1.051(9)
K-	T4	0.06515(5)	0.29789(5)	0.4134(1)	1.04(1)
Rb-	T4	0.06550(8)	0.29958(8)	0.4141(2)	0.93(2)
Na-	T5	0	0.21311(5)	0	1.01(1)
K-	T5	0	0.21625(7)	0	1.16(2)
Rb-	T5	0	0.2185(1)	0	1.02(3)
Na-	O1	0.3058(2)	0	0.5423(4)	2.21(4)
K-	O1	0.3052(2)	0	0.5475(5)	2.60(7)
Rb-	O1	0.3019(4)	0	0.5427(9)	2.4(1)
Na-	O2	0.2323(1)	0.1181(1)	0.6157(3)	1.98(3)
K-	O2	0.2302(2)	0.1192(1)	0.6140(4)	2.24(4)
Rb-	O2	0.2300(2)	0.1205(2)	0.6130(5)	1.77(7)
Na-	O3	0.1811(1)	0.1545(1)	-0.1177(3)	2.27(3)
K-	O3	0.1858(2)	0.1555(1)	-0.1084(3)	2.15(5)
Rb-	O3	0.1838(3)	0.1567(2)	-0.1108(5)	1.92(7)
Na-	O4	0.2387(1)	0.1072(1)	0.2539(3)	1.98(3)
K-	O4	0.2321(2)	0.1018(1)	0.2510(3)	1.99(4)
Rb-	O4	0.2305(3)	0.1019(2)	0.2488(5)	1.94(7)
Na-	O5	0	0.3242(2)	1/2	2.39(5)
K-	O5	0	0.3272(2)	1/2	2.69(7)
Rb-	O5	0	0.3291(3)	1/2	2.1(1)
Na-	O6	0.0818(1)	0.1587(1)	0.0646(3)	1.63(3)
K-	O6	0.0814(1)	0.1624(1)	0.0624(3)	1.76(4)
Rb-	O6	0.0811(2)	0.1646(2)	0.0615(5)	1.64(7)
Na-	O7	0.3717(1)	0.2666(1)	0.4541(3)	2.82(3)
K-	O7	0.3789(2)	0.2709(2)	0.4521(4)	2.56(4)
Rb-	O7	0.3787(2)	0.2688(2)	0.4542(5)	2.16(7)
Na-	O8	0.0079(1)	0.2666(1)	0.1831(3)	2.27(3)
K-	O8	0.0086(2)	0.2695(1)	0.1843(3)	2.30(4)
Rb-	O8	0.0089(2)	0.2723(2)	0.1837(5)	2.05(7)
Na-	O9	0.2099(1)	0.2551(1)	0.1765(3)	1.68(3)
K-	O9	0.2160(1)	0.2504(1)	0.1968(3)	1.91(4)
Rb-	O9	0.2165(2)	0.2506(2)	0.1966(6)	1.95(7)
Na-	O10	0.1148(1)	0.3719(1)	0.3973(3)	2.03(3)
K-	O10	0.1211(1)	0.3687(1)	0.4101(3)	2.04(4)
Rb-	O10	0.1215(2)	0.3708(2)	0.4143(6)	2.04(7)

In the subsequently exchanged K and Rb samples no Ca was analyzed whereas traces of Ca were still found in the Cs-exchanged heulandite.

Na-, K-, and Rb-exchanged heulandite were refined in space group $C2/m$ and refinements converged to R values of 3.8, 3.0, and 4.9%, respectively. Atomic coordinates of framework atoms for the three $C2/m$ heulandites are given in Table 2. Table 3 displays cation and H_2O positions within the structural pores. The X-ray diffraction pattern of Cs-exchanged heulandite indicated that many reflections of the type $h\,k\,l$ were not equivalent to $h\,-k\,l$ reflections, thus ruling out monoclinic symmetry in spite of the pseudo-monoclinic cell dimensions. Cs-exchanged heulandite was refined in space group $C\bar{1}$ leading to an R value of 3.4%. Tables 4 and 5 show atomic coordinates of the framework, channel cations, and H_2O molecules. Table 6 displays cation–oxygen distances of the channel occupants for all exchanged heulandites.

The unit cell parameters of exchanged heulandites varied with the variation of radii of exchanged cations (Table 1). The length of b increased as the radii of exchanged cations increased. Compared with the b length of Na-exchanged heulandite, the b values of K-, Rb-, and Cs-exchanged heulandite increased 0.003, 0.076, and 0.164 Å, respectively. The values of a, c, and β also varied with exchanged cation size but these differences are not so regular as observed for b.

H_2O molecules (21.5, 19.0, 17.5, and 12.7 pfu) were located in the structures of Na-, K-, Rb-, and Cs-exchanged heulandite, respectively. Cs-exchanged heulandite revealed the lowest H_2O concentration relative to the other exchanged heulandite samples. It is obvious that as the radii of exchanged cations increase, the number of H_2O molecules decreases as there is not enough space in the structural pores. In addition, the positive charge of large channel cations is to a higher degree balanced by direct contacts to framework oxygen atoms.

CATION DISTRIBUTIONS IN EXCHANGED HEULANDITE

In general there are four main cation positions (II-1, *A*2, *C*3, and *B*4) in alkali-cation-exchanged heulandite (Fig. 1). II-1, *C*3, and *B*4 were found for Na- and K-exchanged heulandite and all four cation sites were located for Rb- and Cs-exchanged heulandite. *A*2, *C*3, and *B*4 are positioned in, above, or below the plane of the respective tetrahedral rings *A*, *C*, and *B*. The cation populations of these three sites sum up to 80% of the total cation population in the exchanged heulandites.

The *B-ring* hosting *B*4 is confined by 2 × O1, 2 × O5, and 4 × O10 and is almost a regular octagon. As the radii of exchanged cations increase from Na^+ to Cs^+, the *B*4 position gradually shifts from the edge to the center of the *B-ring*. Positional disorder of the *B*4 site was found for K- and Rb-exchanged heulandite. The disorder is mainly along the *c* axis. In Rb-exchanged heulandite the distance between two disordered sites is about 2.3 Å. The main portion (pop. = 33%) remains in the *B-ring*. In K-exchanged heulandite, the distances among the disordered

TABLE 3
Cation and H_2O Positional Parameters and B_{eq} (Å^2) for Na-, K-, and Rb-Exchanged Heulandite at 100 K (Standard Deviations in Parentheses)

	atom	population	x/a	y/b	z/c	Beq
Na-heulandite	Na1 (II-1)	0.13	0.025(2)	-0.091(2)	0.481(4)	8.0(6)
	Na3 (*C*3)	0.58	0.179(2)	0	0.676(2)	2.6(1)
	Na4 (*B*4)	0.29	0.0358(5)	0.485(1)	0.250(3)	3.3(3)
	Ca1 (*C*3)	0.22	0.156(4)	0	0.680(3)	3.6(2)
	Ca2 (*B*4)	0.16	0.5420(5)	0	0.194(3)	1.4(2)
	W1	0.96	0.2203(3)	1/2	-0.0155(7)	3.53(8)
	W2	0.66	0.4264(4)	0.0745(6)	0.0244(9)	4.1(1)
	W3	0.34	0.083(2)	0	0.873(7)	12.07(3)
	W4	1.00	0	1/2	1/2	8.0(3)
	W5	0.33	0.0606(4)	-0.0376(5)	0.708(1)	3.6(2)
	W6	0.58	0.0938(4)	0	0.285(1)	3.4(2)
	W7	0.14	0.418(1)	0.459(2)	0.643(5)	4.9(6)
	W8	0.24	-0.092(1)	0.601(1)	0.090(4)	4.7(3)
	W9	0.16	0.067(4)	0	0.15(1)	7.90*
	W10	0.07	0.219(9)	0	0.90(2)	7.90*
K-heulandite	K1 (II-1)	0.26	0.0101(6)	-0.0967(4)	0.413(1)	12.3(3)
	K3 (*C*3)	0.90	-0.2448(1)	1/2	-0.0582(3)	2.29(4)
	K3' (*C*3)	0.06	0.290(2)	0	0.048(6)	3.8(8)*
	K4 (*B*4)	0.44	0.0290(2)	1/2	0.1708(6)	3.47(8)
	K4' (*B*4)	0.10	0.013(1)	1/2	0.425(4)	3.95*
	K4'' (*B*4)	0.16	1/2	0	1/2	3.95*
	W1	0.18	0.089(2)	0	0.018(4)	4.2(8)*
	W2	1.00	0.3991(2)	-0.0930(2)	0.0461(6)	6.29(9)
	W3	0.73	-0.0811(5)	0	0.216(1)	6.5(2)
	W4	0.16	0	0	0	1.7(16)*
	W5	0.98	0.0753(4)	0	0.183(1)	4.1(2)
	W6	0.12	0.513(2)	0	0.318(5)	0.9(8)*
	W7	0.14	0.021(4)	0	0.07(1)	1.6(12)*
	W8	0.18	0.104(3)	0	0.480(7)	9.7(18)*
	W9	0.12	0	0.459(4)	0.02(4)	9.67(9)*
	W10	0.17	-0.138(1)	0	0.316(2)	0.9(5)*
Rb-heulandite	Rb1 (II-1)	0.15	0.0060(6)	-0.1029(5)	-0.585(2)	8.9(3)
	Rb2 (*A*2)	0.28	-0.0693(4)	0	0.825(2)	5.4(3)
	Rb2' (*A*2)	0.11	0.083(1)	0	0.245(2)	3.95*
	Rb3 (*C*3)	0.89	-0.2491(1)	1/2	-0.0657(3)	1.76(3)
	Rb3' (*C*3)	0.04	0.287(3)	0	0.024(8)	3.95*
	Rb4 (*B*4)	0.33	-0.0003(3)	1/2	0.5637(6)	5.2(1)
	Rb4' (*B*4)	0.16	0.0299(4)	1/2	0.158(1)	4.8(2)
	W1	0.20	0.091(4)	0	0.010(9)	7.90*
	W2	1.00	0.4071(5)	-0.0908(5)	0.048(1)	10.2(2)
	W3	0.81	-0.065(1)	0	0.250(3)	9.7(5)
	W4	0.27	0	0.543(2)	0	5.1(9)
	W5	0.19	-0.066(2)	0.042(2)	0.693(5)	5.02(7)*
	W6	0.38	-0.1394(7)	0	0.313(2)	0.7(3)*
	W7	0.30	-0.018(2)	0	0.947(2)	0.9(5)*

Note. Starred atoms with standard deviation were refined isotropically. Starred atoms without standard deviation were refined with fixed isotropic displacement parameters. Anisotropically refined atoms are given in the form of the isotropic equivalent thermal parameter defined as $B_{eq} = 8/3\ \pi^2\ \Sigma_i\ (\Sigma_j\ (U_{ij}\ a_i^*\ a_j^*\ a_i \cdot a_j))$.

sites are about 2.0 ~ 2.7 Å, and the main portion (pop. = 44%) of *B*4 shifts above or below the plane of the *B-ring*.

*C*3 situates in another eight-membered ring (*C-ring*) forming the type C channel. The *C-ring* is confined by 2 × O1, 2 × O2, 2 × O3, and 2 × O4 and is slightly compressed parallel to the *b* axis (Fig. 2a and 2b). The shape of the *C-ring* is more or less like a boat where O1 sites form the prow and stern. O1, O2, and O4 are coordinated to T2 which has the highest Al population as assumed from the longest average T–O distance in the heulandite structure.

TABLE 4
Framework Positional Parameters of Cs-Exchanged Heulandite

atom	x/a	y/b	z/c	Beq
T1	0.17853(7)	0.16966(7)	0.0983(2)	0.86(2)
T11	0.17828(7)	0.82858(7)	0.0960(2)	0.85(2)
T2	0.28386(8)	0.08912(7)	0.4910(2)	0.84(2)
T21	0.28449(8)	0.91038(7)	0.4908(2)	1.01(2)
T3	0.29198(8)	0.30874(7)	0.2860(2)	0.87(2)
T31	0.29229(7)	0.69228(7)	0.2865(2)	0.79(2)
T4	0.06757(8)	0.29865(7)	0.4170(2)	0.93(2)
T41	0.06688(7)	0.69985(7)	0.4197(2)	0.86(2)
T5	0.00070(8)	0.21926(7)	-0.0026(2)	1.10(2)
O1	0.2989(2)	0.0014(2)	0.5329(5)	1.88(6)
O2	0.2332(2)	0.1206(2)	0.6132(5)	1.60(6)
O21	0.2305(2)	0.8777(2)	0.6132(5)	1.50(6)
O3	0.1895(2)	0.1561(2)	0.8953(5)	1.98(7)
O31	0.1858(3)	0.8403(2)	0.8877(5)	2.17(7)
O4	0.2278(2)	0.1020(2)	0.2494(5)	1.99(7)
O41	0.2298(2)	0.8956(2)	0.2431(5)	2.11(7)
O5	-0.0016(2)	0.3254(2)	0.4936(5)	1.81(6)
O6	0.0799(2)	0.1631(2)	0.0486(5)	1.91(7)
O61	0.0807(2)	0.8346(2)	0.0521(6)	2.14(7)
O7	0.3783(2)	0.2707(2)	0.4514(5)	2.09(6)
O71	0.3742(2)	0.7339(2)	0.4485(5)	2.32(7)
O8	0.0160(2)	0.2749(2)	0.1834(5)	2.35(7)
O81	0.0130(2)	0.7286(2)	0.1946(5)	2.16(7)
O9	0.2152(2)	0.2492(2)	0.1984(5)	1.82(6)
O91	0.2144(2)	0.7483(2)	0.1924(5)	1.88(7)
O10	0.1245(2)	0.3714(2)	0.4338(6)	2.12(7)
O101	0.1195(2)	0.6283(2)	0.4200(6)	2.03(7)

This means that a cation position in the *C-ring* is ideal to compensate the negative charge on the ring walls. Consequently, *C*3 in exchanged heulandite has always the highest cation population. For K-, Rb-, and Cs-exchanged heulandite, an additional *C*3′ cation site very close to *C*3 (0.5 ~ 0.7 Å) was found. Although cation populations of the *C*3′ site are relatively low (4 ~ 14%), the total population of two sites (*C*3 and *C*3′) would be beyond 100% if *C*3′ is assigned to H_2O. Thus the *C*3′ site must be a cation position. The total population of *C*3 and *C*3′ is around 90%.

The ten-membered *A-ring* which determines the channel A is confined by 2 × O2, 4 × O4, and 4 × O6. Four O6 atoms form a plane and two sets of O1 and 2 × O4 situate above and below the plane, respectively. The whole ring viewed edgewise resembles the letter z. *A*2 situates close to 2 × O4 and 2 × O6. The *A*2 site is only populated in Rb- and Cs-exchanged heulandite, thus it is obvious that the *A*2 position is suitable for large cations. An *A*2′ cation site was also located only 0.5 ~ 0.8 Å apart from *A*2, so they cannot be occupied simultaneously. For the same reason as discussed for *C*3′, Cs^+ was assigned to *A*2′. In the case of Rb-exchanged heulandite, there is no excess population if H_2O is assigned to *A*2′. Nevertheless, we still assigned Rb^+ to it because the coordinates of this site are similar to the one of *A*2′ in Cs-exchanged heulandite and in better agreement with the cation composition obtained from electron microprobe analysis and stoichiometry arguments. The total population of *A*2 and *A*2′ is about 40 ~ 50%.

The observed cation disorder phenomena seem to reflect

TABLE 5
Cation and H_2O Positional Parameters and B_{eq} (Å^2) for Cs-Exchanged Heulandite at 100 K (Standard Deviations in Parentheses)

atom	population	x/a	y/b	z/c	Beq
Cs1 (II-1)	0.14	0.4950(2)	0.5982(3)	0.570(2)	4.5(1)
Cs11 (II-1)	0.14	-0.4968(3)	0.5990(3)	-0.558(2)	7.0(2)
Cs2 (*A*2)	0.35	-0.0686(1)	0.0061(2)	-0.2657(5)	4.02(5)
Cs2' (*A*2)	0.14	0.0530(5)	-0.0017(2)	0.151(2)	5.6(2)
Cs3 (*C*3)	0.75	-0.2369(6)	0.49921(8)	-0.0530(9)	1.65(5)
Cs3' (*C*3)	0.14	-0.204(4)	0.5010(4)	-0.006(5)	2.4(3)
Cs4 (*B*4)	0.42	0.0058(2)	0.5007(2)	0.5414(2)	2.62(4)
Ca (B4)	0.10	-0.0489(7)	0.4997(6)	-0.196(2)	2.1(3)*
W1	0.39	0	0	0	3.95*
W2	1.00	-0.0720(5)	0.4144(4)	0.028(1)	9.4(2)
W21	1.00	-0.0776(5)	0.5874(4)	0.034(1)	10.0(2)
W3	0.16	-0.072(2)	-0.008(3)	-0.781(5)	3.95*
W3'	0.15	-0.063(2)	0.039(2)	-0.751(5)	3.95*
W3''	0.13	-0.057(2)	-0.044(3)	0.283(6)	3.95*
W4	0.23	-0.126(1)	0.003(1)	-0.691(3)	3.95*
W7	0.31	0.057(1)	0.026(2)	0.289(3)	3.95*

Note. Starred atoms with standard deviation were refined isotropically. Starred atoms without standard deviation were refined with fixed isotropic displacement parameters. Anisotropically refined atoms are given inthe form of the isotropic equivalent thermal parameter defined as $B_{eq} = 8/3\ \pi^2 \sum_i (\sum_j (U_{ij}\ a_i^*\ a_j^*\ a_i \cdot a_j))$.

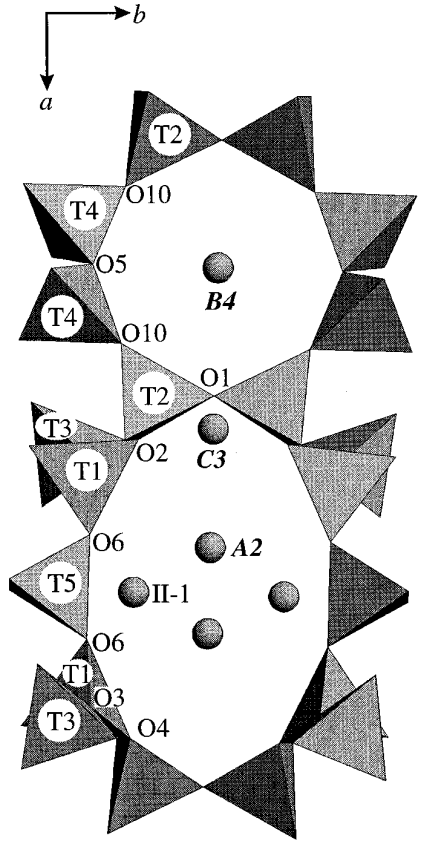

FIG. 1. Tetrahedral model of exchanged heulandite projected parallel to the (001) plane, showing the distributions of cations in channels.

TABLE 6
Cation–Oxygen Distances (Å) for Exchanged Heulandites

Bond	B.L.	bond	B.L.	bond	B.L.	bond	B.L.
Na3-O1	2.83(3)	K3-O2	3.115(3)	Rb3-O2	3.119(4)	Cs3-O2	3.178(6)
Na3-O2	2.44(1)	K3-O2	3.115(3)	Rb3-O2	3.119(4)	Cs3-O21	3.174(6)
Na3-O2	2.44(1)	K3-O3	3.002(3)	Rb3-O3	3.023(4)	Cs3-O3	3.082(5)
Na3-O3	3.156(8)	K3-O3	3.002(3)	Rb3-O3	3.023(4)	Cs3-O31	3.130(5)
Na3-O3	3.156(8)	K3-O4	3.090(3)	Rb3-O4	3.108(4)	Cs3-O41	3.134(6)
Na3-W1	2.35(1)	K3-O4	3.090(3)	Rb3-O4	3.108(4)	Cs3-O4	3.186(6)
Na3-W6	2.61(1)	K3-W2	2.846(3)	Rb3-W2	2.996(6)	Cs3-W2	3.128(9)
		K3-W2	2.846(3)	Rb3-W2	2.996(6)	Cs3-W21	3.057(9)
		K3-W3	2.766(5)	Rb3-W3	2.95(1)	Cs3-W3	3.07(2)
Na4-O1	2.54(1)	K4-O1	2.748(4)	Rb4-O5	3.115(6)	Cs4-O5	3.156(5)
Na4-O10	2.44(2)	K4-O10	2.966(3)	Rb4-O5	3.115(6)	Cs4-O5	3.188(5)
Na4-O10	2.89(2)	K4-O10	2.966(3)	Rb4-O10	3.216(4)	Cs4-O101	3.319(4)
Na4-W2	2.49(2)	K4-W2	2.651(3)	Rb4-O10	3.216(4)	Cs4-O10	3.340(4)
Na4-W2	2.64(2)	K4-W2	2.651(3)	Rb4-W2	3.081(9)	Cs4-O101	3.432(4)
Na4-W2	2.89(2)	K4-W2	2.957(4)	Rb4-W2	3.081(9)	Cs4-O10	3.473(4)
Na4-W8	2.55(2)	K4-W2	2.957(4)	Rb4-W4	3.320(9)	Cs4-W21	3.253(7)
				Rb4-W4	3.320(9)	Cs4-W2	3.272(7)
Na1-O2	3.37(1)	K1-O3	3.362(8)	Rb1-O3	3.260(9)	Cs1-O3	3.399(8)
Na1-O3	3.23(3)	K1-O6	3.373(9)	Rb1-O6	3.36(1)	Cs1-O6	3.41(1)
Na1-O7	3.04(2)	K1-O7	2.958(8)	Rb1-O7	2.950(9)	Cs1-O7	3.315(5)
Na1-W3	2.96(5)	K1-O7	3.416(7)	Rb1-O7	3.327(9)	Cs1-O71	3.126(6)
Na1-W3	3.09(5)	K1-W3	3.02(1)	Rb1-W1	3.39(5)	Cs1-W3	3.04(4)
Na1-W5	2.76(3)	K1-W5	2.987(9)	Rb1-W3	2.90(2)	Cs1-W7	3.05(2)
Na1-W5	2.78(3)	K1-W7	3.15(6)	Rb1-W5	3.04(3)		
Na1-W6	2.80(3)	K1-W8	3.02(2)	Rb1-W5	3.06(3)	Cs11-O31	3.36(1)
Na1-W7	2.81(3)	K1-W10	2.86(1)	Rb1-W6	2.98(1)	Cs11-O61	3.51(2)
Na1-W7	2.88(4)	K1-W10	2.96(1)	Rb1-W6	2.98(1)	Cs11-O7	3.021(7)
				Rb1-W7	3.34(2)	Cs11-O71	3.367(6)
						Cs11-W3'	3.24(4)
						Cs11-W7	3.47(3)
				Rb2-O4	3.229(4)	Cs2-O61	3.345(5)
				Rb2-O4	3.229(4)	Cs2-O41	3.441(5)
				Rb2-O6	3.113(5)	Cs2-O4	3.478(4)
				Rb2-O6	3.113(5)	Cs2-O6	3.505(5)
				Rb2-W3	3.12(2)		
				Rb2-W5	3.39(3)		
				Rb2-W5	3.39(3)		
				Rb2-W6	3.43(2)		

Note. Only cation–oxygen distances for highly populated channel cation position are given.

Si, Al disorder within the framework and are governed by the interaction of cations with the framework.

II-1 situates in cage II which is formed by two *A-rings* and two *C-rings*. In all four exchanged heulandite the II-1 position was refined. The population of the II-1 site is around 13 ~ 26%. In general, cations on II-1, which exhibit only a weak interaction with the tetrahedral framework, display the largest displacement parameters. Similar arguments hold for the *A*2 position.

In our K-exchanged heulandite K^+ preferentially occupies *C*3 and *B*4 which agrees with the results of Galli *et al.* (6). However, it is difficult to decide whether K^+ occupies II-1 or *A*2. Galli *et al.* assigned K^+ to *A*2. Whereas, we assigned K^+ to II-1 based on a partial dehydration experiment accompanied with a subsequent crystal-structure refinement: partial dehydration of K-exchanged heulandite at 293 K in dry nitrogen for 5 h shows that the population of *A*2 dropped dramatically and the population of II-1 remains unchanged. Our four main cation sites in Cs-exchanged heulandite are in agreement with Petrov *et al.*'s result (8) and the disordered cation sites support conclusions by Smyth *et al.* (7). Na^+ in the *C*3 and *B*4 sites are in agreement with Gunter *et al.*'s assignment (12). However, in this study Na^+ was assigned to II-1 instead of *A*2 which is in better agreement with the cation composition obtained from electron microprobe analysis. It must be noted again that it is very difficult to decide whether a partially occupied channel site is populated by H_2O or Na^+

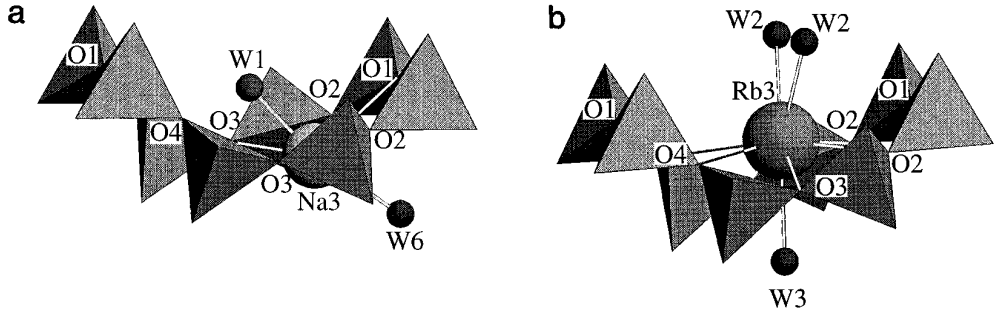

FIG. 2. Oxygen coordination polyhedra of the *C*3 site. (a) Oxygen coordination of Na^+ on the *C*3 site. (b) Oxygen coordination of Rb^+ on the *C*3 site.

because both species have very similar scattering factors for X rays. In addition, dehydration experiments (13–15) are not very decisive as loss of channel H_2O accompanies channel cation diffusion. For this reason the assignment was done following the general trend from Cs to Na.

CATION COORDINATIONS IN EXCHANGED HEULANDITE

Because the radius of Na^+ is only ca. 1.16 Å (22), Na^+ on the *C*3 site shifts toward the cavity wall of the channel C. Na^+ on *C*3 bonds five oxygen atoms of the framework (O1, 2 × O2 and 2 × O3). One of the disordered H_2O sites (W6, W7) coordinates Na^+ on the one side and W1 completes the coordination (Fig. 2a) on the opposite side (low populated H_2O sites are ignored). With increasing cation radii from Na^+ to Cs^+, the *C*3 site shifts from the bottom of the boat to the center of it. For K-, Rb-, and Cs-exchanged heulandite, cations occupying *C*3 bond to six oxygen atoms of the framework (2 × O2, 2 × O3, and 2 × O4, or O*i* with its pseudo-mirror plane related position O*i*1 for Cs-exchanged heulandite, $i = 2, 3, 4$). Two W2 situated above the *C-ring* are in reasonable distances to coordinate *C*3 in K-, Rb-, and Cs-exchanged heulandites. Below the *C-ring* there are two H_2O positions (W1 and W3) to coordinate *C*3 for K- and Rb-exchanged heulandite. However, the distance between W1 and W3 is only 1.7 Å, thus they cannot exist simultaneously. In Cs-exchanged heulandite, three low populated H_2O sites (W3, W3′, and W3″) were refined below the ring. Because they are again very near to each other (0.8 ~ 0.9 Å), a disordered distribution must be assumed. The total population of three sites (W3, W3′, and W3″) is about 44%, thus only half of Cs^+ in the *C*3 site (pop. ≈ 90%) shows this type of coordination. Occupancy of one of the W3 sites below the ring may depend on whether II-1 or *A*2 is occupied in Cs-exchanged heulandite. The space between *C*3 and II-1 or *C*3 and *A*2 in Cs-exchanged heulandite is not large enough to incorporate an additional H_2O molecule. The coordination of Rb^+ on *C*3 is shown in Fig. 2b.

*A*2 bonds to four oxygen atoms of the framework (2 × O4, 2 × O6, or O*i* and O*i*1 for Cs-exchanged heulandite, $i = 4, 6$). There is no H_2O in a reasonable distance to *A*2 in Cs-exchanged heulandite. In Rb-exchanged heulandite Rb^+ on the *A*2 site bonds to two W5 on the one side and to one of the disordered H_2O molecules (W3 or W6) on the other side.

The coordination of *B*4 varies along with the variation of cation radii. In Na-exchanged heulandite *B*4 shifts more or less toward the cavity wall of the channel B. Na^+ on the *B*4 site is coordinated by three oxygen atoms of the framework (O1, 2 × O10). Four H_2O molecules (3 × W2, W8) are in reasonable distances to Na^+ on *B*4 (Fig. 3a). K^+ on *B*4 shifts not only toward the wall of the cavity of

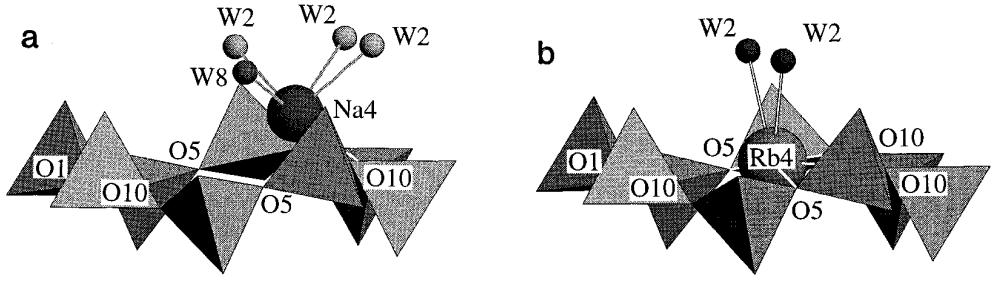

FIG. 3. Oxygen coordination polyhedra of the *B*4 site. (a) Oxygen coordination of Na^+ on the *B*4 site. (b) Oxygen coordination of Rb^+ on the *B*4 site.

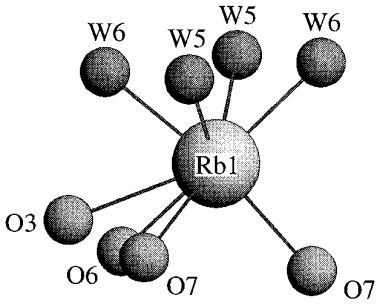

FIG. 4. Oxygen coordination polyhedron of Rb^+ on the II-1 site. II-1 is in the cage II. Cations on this site bond oxygen atoms of the framework on the one side and H_2O molecules on the other side.

TABLE 7
T–O Distances (Å) of Na-Exchanged Heulandite

bond	B.L.	A.B.L.	Al%	bond	B.L.	A.B.L.	Al%
T1-O4	1.628(2)			T2-O1	1.642(1)		
T1-O3	1.629(2)	1.634	23	T2-O2	1.664(1)	1.660	42
T1-O9	1.634(2)			T2-O10	1.665(1)		
T1-O6	1.644(1)			T2-O4	1.670(1)		
T3-O7	1.622(2)			T4-O7	1.610(2)		
T3-O2	1.632(2)	1.631	20	T4-O10	1.627(2)	1.624	15
T3-O3	1.633(2)			T4-O8	1.627(2)		
T3-O9	1.635(2)			T4-O5	1.630(1)		
T5-O8	1.618(2)						
T5-O8	1.618(2)	1.624	15				
T5-O6	1.629(1)						
T5-O6	1.629(1)						

Note. B.L., bond length; A.B.L., average bond length.

the channel B but also out of the plane of the *B-ring*. K^+ on the *B*4 site bonds to three oxygen atoms of the framework (O1, 2 × O10) and four H_2O molecules (4 × W2). In Rb- and Cs-exchanged heulandite the *B*4 site is situated almost in the middle of the *B-ring*; cations on this site bond to four oxygen atoms of the framework (2 × O5 and 2 × O10, or O5, O51, O10, and O101 for Cs-exchanged heulandite) and two H_2O molecules (2 × W2). For Rb-exchanged heulandite, two W4 are also in reasonable distances to coordinate Rb^+ on *B*4, however, the population of W4 is relatively low (27%). Figure 3b shows the coordination of Rb^+ on *B*4.

H_2O molecules in cage II are highly disordered. Na^+ on II-1 bonds three oxygen atoms of the framework (O2, O3, and O7) and seven H_2O molecules (2 × W3, 2 × W5, W6, and 2 × W7) are in reasonable distances to the cation. However, the distance between W3 and W5 is ca. 1.3 Å, and the distance between W6 and W7 is ca. 1 Å, thus, only three or four H_2O molecules can coordinate Na^+ on the II-1 site. For K-, Rb-, and Cs-exchanged heulandite cations in the II-1 site are surrounded by four oxygen atoms of the framework (O3, O6, and 2 × O7, or O*i* and O*i*1, for Cs-exchanged heulandite $i = 3, 6, 7$) on the one side. Three or four H_2O molecules can coordinate K^+ and Rb^+ on II-1 on the other side. Only two H_2O molecules are in reasonable distances to coordinate Cs^+ on the II-1 site. Figure 4 displays the coordination of Rb^+ on II-1.

Si, Al ORDERING IN HEULANDITE FRAMEWORK

The results of the refinement show that the Na-, K-, and Rb-exchanged heulandite have almost the same framework structure as evaluated from structural parameters (Table 2). The Si/Al ratio of the tetrahedra (Tables 7 and 8) was estimated from the mean T–O distances (23). The results were subsequently normalized to the Al concentration measured by electron microprobe analysis. The highest portion of Al occurs on T2 (42%), and the lowest on T4 and T5 (15%). However, the framework of Cs-exchanged heulandite shows some significant differences. The highest portion of Al occurs on T21 (68%), whereas, the share of Al on T2 is only 25% which is the pseudo-mirror plane related position to T21. Moreover, T3 and T4 show a significantly higher Al content than T31 and T41. The Al content in T3 and T4 is more than four times of that in T31 and T41 (Table 8). Tables 9 and 10 display T–O–T and O–T–O angles in exchanged heulandites.

There has been a long standing discussion about the true symmetry of heulandite. The first refinement of heulandite (2) was performed in the acentric space group *Cm*. Most other authors (3, 6–15) selected the space group *C*2/*m* mainly to avoid correlation problems of pseudo-symmetry related sites in the last squares refinement. Armbruster and Gunter (14), investigating dehydration of a heulandite type zeolite, performed a second harmonic generation test

TABLE 8
T–O Distances (Å) of Cs-Exchanged Heulandite

Bond	B.L	A.B.L.	Al%	Bond	B.L.	A.B.L.	Al%
T1-O9	1.619(4)			T11-O41	1.619(4)		
T1-O3	1.621(3)	1.625	18	T11-O61	1.622(2)	1.622	16
T1-O6	1.628(2)			T11-O91	1.623(4)		
T1-O4	1.633(4)			T11-O31	1.624(3)		
T2-O1	1.617(4)			T21-O1	1.675(4)		
T2-O10	1.634(3)	1.633	25	T21-O41	1.684(4)	1.684	68
T2-O2	1.637(3)			T21-O101	1.689(3)		
T2-O4	1.644(3)			T21-O21	1.689(3)		
T3-O9	1.632(3)			T31-O21	1.606(3)		
T3-O7	1.640(3)	1.640	31	T31-O91	1.610(3)	1.611	7
T3-O2	1.641(3)			T31-O71	1.611(3)		
T3-O3	1.646(3)			T31-O31	1.617(3)		
T4-O7	1.624(4)			T41-O101	1.599(3)		
T4-O8	1.626(4)	1.629	22	T41-O81	1.607(4)	1.608	4
T4-O10	1.629(3)			T41-O71	1.609(4)		
T4-O5	1.638(3)			T41-O5	1.618(3)		
T5-O8	1.634(4)						
T5-O81	1.637(4)	1.639	30				
T5-O6	1.642(3)						
T5-O61	1.643(3)						

Note. B.L., bond length; A.B.L., average bond length.

TABLE 9
T–O–T and O–T–O Angles (°) in Na-Exchanged Heulandite

	angle(°)		angle(°)		angle(°)
O4-T1-O3	107.05(10)	O1-T2-O2	107.40(11)	O7-T3-O2	109.60(10)
O4-T1-O9	112.51(9)	O1-T2-O10	105.02(10	O7-T3-O3	108.99(8)
O4-T1-O6	108.35(8)	O1-T2-O4	110.64(12)	O7-T3-O9	111.09(10)
O3-T1-O9	111.62(10)	O2-T2-O10	111.59(9)	O2-T3-O3	105.44(10)
O3-T1-O6	108.21(9)	O2-T2-O4	110.79(8)	O2-T3-O9	110.29(7)
O9-T1-O6	108.96(7)	O10-T2-O4	111.19(9)	O3-T3-O9	111.26(9)
O7-T4-O10	112.05(9)	O8-T5-O8	107.22(12)		
O7-T4-O8	109.96(11)	O8-T5-O6	112.04(9)		
O7-T4-O5	112.07(10)	O8-T5-O6	109.57(7)		
O10-T4-O8	108.58(10)	O8-T5-O6	109.57(7)		
O10-T4-O5	106.42(12)	O8-T5-O6	112.04(9)		
O8-T4-O5	107.57(5)	O6-T5-O6	106.46(9)		
T2-O1-T2	157.75(19)	T4-O5-T4	145.87(22)	T5-O8-T4	148.66(10)
T3-O2-T2	144.45(12)	T5-O6-T1	134.65(12)	T1-O9-T3	144.86(9)
T1-O3-T3	143.94(15)	T4-O7-T3	163.36(16)	T4-O10-T2	141.38(13)
T1-O4-T2	140.77(12)				

which indicated that this sample was centric thus justifying refinement in space group $C2/m$. However, it should be noted that there is only little experience on the sensitivity of such second harmonic generation tests in case of structures which possess a centric topology with the acentricity caused by minor preferred Si, Al distribution within the tetrahedral framework.

We must assume that treatment of a natural heulandite in chloride solutions at temperatures below 423 K does not change the Si, Al distribution in the framework. Therefore, it was surprizing when we found in this study that the X-ray diffraction pattern of Na-, K-, and Rb-exchanged heulandite was in agreement with $C2/m$ symmetry but that of Cs-exchanged heulandite indicated $C\bar{1}$ symmetry. Two Cs-exchanged heulandites were studied. For one crystal (crystal 1) a full sphere of diffraction data was collected up to $\theta = 15°$ and a half sphere up to $\theta = 25°$. For the second crystal (crystal 2) a full sphere up to $\theta = 25°$ was collected. Both crystals revealed the same characteristics: many reflections of the type $h\,k\,l$ were not equivalent to $h\,-k\,l$ reflections thus ruling out monoclinic symmetry in spite of the pseudo-monoclinic cell dimensions. This discrepancy was especially strong for crystal 1 leading to an agreement factor of only 7.9% when averaging intensities according to $C2/m$ symmetry. The corresponding agreement factor for crystal 2 was considerably better (4.3%) but the same reflections as for crystal 1 showed the most dramatic deviations for $h\,k\,l$ and $h\,-k\,l$. For this reason the structures of Cs-exchanged heulandite were refined in the triclinic space group $C\bar{1}$. As shown above, subsequent refinements lead to pronounced Si, Al ordering which is considerably stronger for crystal 1 compared to crystal 2. After this finding a full sphere of diffraction data

TABLE 10
T–O–T and O–T–O Angles (°) in Cs-Exchanged Heulandite

	angle(°)		angle(°)		angle(°)
O9-T1-O3	112.04(17)	O1-T2-O10	107.76(16)	O9-T3-O7	111.48(18)
O9-T1-O6	110.03(15)	O1-T2-O2	108.78(16)	O9-T3-O2	110.41(14)
O9-T1-O4	111.33(18)	O1-T2-O4	108.65(19)	O9-T3-O3	111.00(18)
O3-T1-O6	109.47(17)	O10-T2-O2	111.41(17)	O7-T3-O2	109.79(17)
O3-T1-O4	106.18(17)	O10-T2-O4	110.43(18)	O7-T3-O3	108.60(14)
O6-T1-O4-	107.63(17)	O2-T2-O4	109.74(16)	O2-T3-O3	105.38(17)
O41-T11-O61	108.82(17)	O1-T21-O41	109.16(18)	O21-T31-O91	110.81(13)
O41-T11-O91	111.96(18)	O1-T21-O101	106.96(16)	O21-T31-O71	110.38(18)
O41-T11-O31	106.79(17)	O1-T21-O21	108.53(16)	O21-T31-O31	106.30(18)
O61-T11-O91	109.44(16)	O41-T21-O101	111.29(17)	O91-T31-O71	110.74(19)
O61-T11-O31	109.01(18)	O41-T21-O21	109.94(15)	O91-T31-O31	110.21(18)
O91-T11-O31	110.75(17)	O11-T21-O21	110.87(16)	O71-T31-O31	108.27(15)
O7-T4-O8	110.29(20)	O101-T41-O81	110.23(19)	O8-T5-O81	106.72(20)
O7-T4-O10	113.21(16)	O101-T41-O71	112.26(16)	O8-T5-O6	112.24(18)
O7-T4-O5	110.99(17)	O101-T41-O5	107.06(17)	O8-T5-O61	110.98(16)
O8-T4-O10	109.61(20)	O81-T41-O71	108.96(20)	O81-T5-O6	110.19(16)
O8-T4-O5	106.97(16)	O81-T41-O5	107.44(15)	O81-T5-O61	111.38(18)
O10-T4-O5	105.51(16)	O71-T41-O5	110.77(17)	O6-T5-O61	105.41(17)
T2-O1-T21	158.50(23)	T11-O41-T21	137.88(23)	T4-O8-T5	150.80(24)
T2-O2-T3	148.47(20)	T41-O5-T4	146.28(24)	T41-O81-T5	152.47(21)
T31-O21-T21	147.26(20)	T1-O6-T5	137.46(23)	T1-O9-T3	149.98(16)
T1-O3-T3	148.25(24)	T11-O61-T5	139.64(24)	T31-O91-T11	148.89(17)
T31-O31-T11	149.77(25)	T4-O7-T3	152.88(22)	T4-O10-T2	150.32(23)
T1-O4-T2	138.03(24)	T41-O71-T31	159.19(25)	T41-O101-T21	145.93(23)

of a second Rb-exchanged heulandite was measured in order to find out whether the same symmetry lowering could be observed for this crystal. As a matter of fact, also for this Rb-exchanged crystal several reflections showed deviations for $h\,k\,1$ and $h\,-k\,l$ type leading to an agreement factor on intensity to 4.3% when averaged in space group $C2/m$. However, when refined in $C\bar{1}$ with all reflections, significant Si, Al ordering could not be found. For Na- and K-exchanged heulandite we also considered lower symmetry by measuring at least twice as many reflections as necessary. However, when symmetry equivalent reflection intensities were averaged in $C2/m$ symmetry, agreement factors of 2.6 and 1.2%, respectively, were obtained. Nevertheless, refinements in $C\bar{1}$ symmetry were tested also for these samples but as expected no deviation from $C2/m$ symmetry with respect to the Si, Al distribution could be resolved.

All results summarized above indicate that Al-rich heulandite may possess space group $C\bar{1}$ due to Si, Al ordering. However, because of the pseudo-monoclinic symmetry there is also a high probability of submicroscopic twinning which will influence the degree of bulk Si, Al ordering as observed in a diffraction experiment which only resolves the average in the crystal. Even for crystals with a low twinning contribution, symmetry lowering can only be resolved from X-ray data when investigated in the form of cation-exchanged samples where the channel cation must be heavy and thus sensitive to the X-ray experiment. In other words, the heavy element in the channels enforces the symmetry information of the framework, where the diffraction contribution of the low symmetry framework alone is not significant enough to be resolved.

REFERENCES

1. G. Gottardi and E. Galli, "Natural Zeolites," p. 256, New York, 1985.
2. A. B. Merkle and M. Slaughter, *Am. Mineral.* **53,** 1120 (1968).
3. A. Alberti, *Tschermaks Min. Petr. Mitt.* **22,** 25 (1975).
4. K. Koyama and Y. Takéuchi, *Z. Kristallogr.* **145,** 216 (1977).
5. F. A. Mumpton, "Natural Zeolite: Occurrence, Properties, Use" (L. B. Sand, and F. A. Mumpton, Eds.), Vol. 3, p. 3–27. Pergamon Press, Oxford, 1978.
6. E. Galli, G. Gottardi, H. Mayer, A. Preisinger, and E. Passaglia, *Acta Crystallogr. Sect. B.* **39,** 189 (1983).
7. J. R. Smyth, A. T. Spaid, and D. L. Bish, *Am. Mineral.* **75,** 522 (1990).
8. O. E. Petrov, L. D. Filizova, and G. N. Kirov, *C. R. Acad. Bulgare Sci.* **44,** 77 (1991).
9. O. E. Petrov, L. D. Filizova, and G. N. Kirov, *C. R. Acad. Bulgare Sci.* **38,** 5 (1985).
10. N. Bresciani-Pahor, M. Calligaris, G. Nardin, L. Randaccio, and E. Russo, *J. Chem. Soc., Dalton Trans.* 1511 (1980).
11. N. Bresciani-Pahor, M. Calligaris, G. Nardin, and L. Randaccio, *J. Chem. Soc., Dalton Trans.* 2288 (1981).
12. M. E. Gunter, Th. Armbruster, Th. Kohler, and C. R. Knowles, *Am. Mineral.* **79,** 675 (1994).
13. A. Alberti and G. Vezzalini, *Tschermaks Min. Petr. Mitt.* **31,** 259 (1983).
14. Th. Armbruster and M. E. Gunter, *Am. Mineral.* **76,** 1872 (1991).
15. Th. Armbruster, *Am. Mineral.* **78,** 260 (1993).
16. T. W. Hambley and J. C. Taylor, *J. Solid State Chem.* **54,** 1 (1984).
17. R. N. Sukheswala, R. K. Avasia, and M. Gangopadhyay, *Mineral. Mag.* **39,** 658 (1974).
18. F. C. Hawthorne and C. Calvo. *J. Solid State Chem.* **22,** 157 (1977).
19. Enraf Nonius, "Structure determination package (SDP)." Enraf Nonius, Delft, the Netherlands, 1983.
20. Siemens, "Shelxtl PC 4.1 (computer program)." Siemens analytical X-ray instruments Incorporation, Madison, WI. 1990.
21. Th. Armbruster, H. B. Bürgi, M. Kunz, E. Gnos, St. Brönnimann, and Ch. Lienert, *Am. Mineral.* **75,** 135 (1990).
22. R. D. Shannon, *Acta Crystallogr. Sect. A.* **32,** 751 (1976).
23. J. B. Jones, *Acta Crystallogr. Sect. B.* **24,** 355 (1968).